



Original Research

Nomogram for preoperative estimation of microvascular invasion risk in hepatocellular carcinoma

Xiao-Wen Huang^{a,b}, Yan Li^b, Li-Na Jiang^b, Bo-Kang Zhao^c, Yi-Si Liu^d, Chun Chen^e, Dan Zhao^b, Xue-Li Zhang^b, Mei-Ling Li^b, Yi-Yun Jiang^b, Shu-Hong Liu^b, Li Zhu^b, Jing-Min Zhao^{a,b,*}

^a Medical School of Chinese PLA, Beijing, China

^b Department of Pathology and Hepatology, The Fifth Medical Center of Chinese PLA General Hospital, Beijing, China

^c Department of Hepatology, Center of Infectious Diseases and Pathogen Biology, The First Hospital of Jilin University, Changchun, China

^d First Department of Liver Disease Center, Beijing Youan Hospital, Capital Medical University, Beijing, China

^e Senior Department of Hepatology, The Fifth Medical Center of Chinese PLA General Hospital, Beijing, China

ARTICLE INFO

Keywords:

Microvascular invasion
Hepatocellular carcinoma
Multivariable logistic regression
Nomogram
Preoperative

ABSTRACT

Microvascular invasion (MVI) is an adverse prognostic indicator of tumor recurrence after surgery for hepatocellular carcinoma (HCC). Therefore, developing a nomogram for estimating the presence of MVI before liver resection is necessary. We retrospectively included 260 patients with pathologically confirmed HCC at the Fifth Medical Center of Chinese PLA General Hospital between January 2021 and April 2024. The patients were randomly divided into a training cohort ($n = 182$) for nomogram development, and a validation cohort ($n = 78$) to confirm the performance of the model (7:3 ratio). Significant clinical variables associated with MVI were then incorporated into the predictive nomogram using both univariate and multivariate logistic analyses. The predictive performance of the nomogram was assessed based on its discrimination, calibration, and clinical utility. Serum carnosine dipeptidase 1 ([CNDP1] OR 2.973; 95 % CI 1.167–7.575; $p = 0.022$), cirrhosis (OR 8.911; 95 % CI 1.922–41.318; $p = 0.005$), multiple tumors (OR 4.095; 95 % CI 1.374–12.205; $p = 0.011$), and tumor diameter ≥ 3 cm (OR 4.408; 95 % CI 1.780–10.919; $p = 0.001$) were independent predictors of MVI. Performance of the nomogram based on serum CNDP1, cirrhosis, number of tumors and tumor diameter was achieved with a concordance index of 0.833 (95 % CI 0.771–0.894) and 0.821 (95 % CI 0.720–0.922) in the training and validation cohorts, respectively. It fitted well in the calibration curves, and the decision curve analysis further confirmed its clinical usefulness. The nomogram, incorporating significant clinical variables and imaging features, successfully predicted the personalized risk of MVI in HCC preoperatively.

Abbreviations

AFP α -fetoprotein
ALT alanine aminotransferase
AST aspartate aminotransferase
CA-125 carbohydrate antigen 125
CA-19-9 carbohydrate antigen 19-9
CEA Carcinoembryonic antigen
CNDP1 carnosine dipeptidase 1
DCA decision curve analysis
GGT γ -glutamyl transpeptidase
HBsAg hepatitis B e antigen

HBsAg hepatitis B surface antigen
HBV hepatitis B virus
HBV DNA hepatitis B virus DNA
HCC hepatocellular carcinoma
HCV hepatitis C virus
HCV RNA hepatitis C virus RNA
LCAT lecithin-cholesterol acyltransferase
MVI microvascular invasion
STIP1 stress induced phosphoprotein 1
PD-L1 programmed cell death 1 ligand 1
PT prothrombin time
RBCs red blood cells

* Correspondence author at: Jing-Min Zhao, Department of Pathology and Hepatology, The Fifth Medical Center of Chinese PLA General Hospital, Beijing, 100039, China.

E-mail address: jmzhao302@163.com (J.-M. Zhao).

<https://doi.org/10.1016/j.tranon.2024.101986>

Received 17 October 2023; Received in revised form 22 April 2024; Accepted 5 May 2024

1936-5233/© 2024 The Authors. Published by Elsevier Inc. This is an open access article under the CC BY-NC-ND license (<http://creativecommons.org/licenses/by-nc-nd/4.0/>).

ROC	receiver operating characteristic
TBil	total bilirubin
WBCs	white blood cells

Introduction

Hepatocellular carcinoma (HCC) is the sixth most prevalent cancer and third leading cause of cancer-related deaths worldwide [1]. Surgical resection and liver transplantation are effective curative treatments for HCC [2,3]. However, the high postoperative recurrence rate in patients with HCC can be as high as 70–80 %, and after liver transplantation, the rate is about 25 % [4,5]. Due to tumor recurrence, the unsatisfactory 5-year overall survival rate of HCC is approximately 10–20 % [6].

Microvascular invasion (MVI) is characterized by a nested distribution of tumor cells within the vessels of the surrounding liver parenchyma [7]. It is considered one of the most significant prognostic factors for HCC, and serves as an indicator of strong tumor invasion [8–10]. In order to improve the prognosis of HCC with MVI, it is recommended to perform anatomic subsegmentectomy or partial hepatectomy with wide margins [11,12]. In addition, considering the scarcity of liver transplantation and the possibility of tumor recurrence, new inclusion criteria for liver transplantation now include the absence of MVI as an essential variable [13].

However, preoperative imaging is not reliable for diagnosing MVI, and only tumor specimens obtained after liver resection or transplantation are considered reliable. Needle biopsy may provide a pathological diagnosis of a hepatic tumor in some cases, but there are not enough samples to perform a meaningful MVI evaluation of HCC. Consequently, the diagnosis of MVI has limited impact on preoperative decision making. Surgical procedures for patients can be chosen based on a risk-benefit assessment with an accurate preoperative estimation of MVI presence.

Over the past decade, many efforts have been made to preoperatively estimate MVI [9,14]. MVI in HCC could be predicted using clinical factors, including age, tumor size, tumor number, differentiation, and α -fetoprotein (AFP) levels in serum [9,15,16]. Furthermore, certain tumor biomarkers including recombinant stress induced phosphoprotein 1 (STIP1), circ-RNAs, lncRNAs and programmed cell death 1 ligand 1 (PD-L1) in HCC patients have been strongly correlated with MVI [17]. Unfortunately, the clinical applicability of these serum markers in preoperative risk estimation of MVI remains to be determined.

Recent studies have shown that certain imaging characteristics, such as capsule formation, irregular tumor margin and increased metabolism hold great potential in predicting MVI [15,18,19]. Qualitative findings, however, have limitations including interobserver variability and lack of validation outside the study.

An increasing amount of evidence has demonstrated that disrupted lipid metabolism is linked to a poor prognosis for HCC following radical treatments [20,21] and can trigger tumor metastasis [22]. However, there is limited understanding of the lipid metabolism-related molecules that regulate HCC metastasis or their potential molecular mechanisms in HCC recurrence. Lecithin-cholesterol acyltransferase (LCAT), a crucial enzyme involved in the extracellular metabolism of plasma lipoproteins, is primarily synthesized in the liver and secreted into the plasma. Here, it catalyzes the conversion of cholesterol and phosphatidylcholines (lecithins) into cholesteryl esters and lysophosphatidylcholines on the surface of high and low density lipoproteins (HDLs and LDLs) [23–25].

In tumor cells, the regulatory mechanisms of the cell cycle are disrupted, leading to an inability for cells to cease growth and division in a normal manner. This results in uncontrolled cell proliferation and ultimately leads to the formation of cancer [26]. Carnosine dipeptidase 1 (CNDP1) is primarily expressed in the brain, liver, and serum [27,28]. This enzyme is classified within the metallopeptidase H family and serves as a proteolytic enzyme with the ability to break down histidine-containing dipeptides, including carnosine and homocarnosine. Its physiological functions include protein degradation,

facilitation of specific protein biochemical activities, tissue regeneration, and regulation of cell cycle progression [29]. Nevertheless, there is a scarcity of studies investigating the involvement of LCAT and CNDP1 in HCC.

Therefore, in order to meet the specific demands of personalized clinical assessment, further investigation is essential for the development of valuable models for predicting MVI in patients with HCC. Among the existing models, the nomogram stands out due to its provision of evidence-based, individualized, and highly accurate risk estimation. We found that LCAT and CNDP1 were expressed at low levels in HCC tissues compared with its expression in the noncancerous liver tissues, and low expression was closely correlated with HCC metastasis and recurrence. We consider the investigation of these two novel biomarkers to be crucial for the diagnosis and treatment of HCC, and believe that it can help bridge existing research gaps.

The aim of this study was to develop and validate a nomogram capable of predicting MVI in HCC before surgery by establishing a correlation between imaging characteristics and laboratory examinations. This nomogram facilitates preoperative assessment of personalized MVI risk and has demonstrated particular effectiveness in guiding therapeutic stratification before surgery.

Materials and methods

Study population

Between January 2021 and April 2024, 260 patients with pathologically confirmed HCC at the Fifth Medical Center of Chinese PLA General Hospital were retrospectively enrolled in this study. The patients were randomly divided into a training cohort ($n = 182$) and a validation cohort ($n = 78$) in a 7:3 ratio. This study was approved by the Institutional Ethics Committee of the Fifth Medical Center of Chinese PLA General Hospital. Informed consent was obtained from all patients for the data to be used in the study. The patients did not receive any financial compensation.

The inclusion criteria were as follows: (1) age > 18 years, (2) histologically confirmed HCC with MVI, (3) receipt of preoperative MRI of the abdomen, (4) routine plasma samples retained in the hospital specimen bank, and (5) well-preserved imaging and clinical data. Patients who were younger than 18 years of age, had a history of other cancers, or had incomplete imaging and clinical data were excluded.

Laboratory examination and histology

The routine preoperative examination included liver and renal function tests, hepatitis B and C immunology, blood ammonia, serum tumor markers combination level (including AFP and carbohydrate antigen 19–9 [CA-19–9], carbohydrate antigen 125 [CA-125]), prothrombin time (PT), and whole blood cell analysis. Demographic information and laboratory examinations were collected from patients' medical records. Serum LCAT and CNDP1 levels were determined by detecting the serum of patients in the hospital specimen bank. Serum LCAT and CNDP1 levels were screened using the Human LCAT (Phosphatidylcholine-sterol acyltransferase) ELISA Kit (EH2111, FineTest, Wuhan, China) and Human CNDP1 ELISA Kit (EK1957, BOSTER, Wuhan, China), respectively. After adding the stop solution to each sample and standard well, absorbance was immediately measured at 450 nm. We then calculated the mean absorbance for each set of duplicate standards and samples, and subtracted the average zero-standard optical density. The standard curve was plotted on a log-log graph, with the standard concentration on the x-axis and absorbance on the y-axis. A best-fit straight line through the standard points was drawn to calculate the plasma sample concentration.

In a 1:1 ratio, specimens were collected from the junction of the tumor and adjacent liver tissues at the 12, 3, 6, and 9 o'clock positions from curative hepatectomy [7]. Two pathologists evaluated the

pathological characteristics of tumor number, Edmondson-Steiner grade, MVI status, and noncancerous liver parenchymal cirrhosis. MVI was defined as the presence of tumor cells within the portal vein, hepatic vein, or a prominent vessel in the hepatic tissue surrounded by the endothelium, which could only be observed under microscopic examination [7,15,30]. The laboratory and clinicopathological variables in this study are reported in Table 1.

MR imaging

All patients underwent preoperative imaging examinations, specifically abdominal magnetic resonance imaging (MRI). Imaging data included the tumor number, tumor diameter, and the presence of cirrhosis, all based on preoperative abdominal MRI. Two experienced radiologists independently evaluated the preoperative imaging data. Disputes over imaging findings were resolved through discussions among radiologists, and a final standardized imaging report was generated for each patient. The imaging information used in this study is presented in Table 1.

Statistical analysis

Continuous variables were tested for normality and expressed as mean ± standard deviation (SD) when conforming to a normal distribution, using a two-tailed T test. If they did not conform to a normal distribution, they were expressed as the median (interquartile range) using the Wilcoxon rank-sum test. Categorical variables were compared using the χ^2 test and are presented as frequencies (percentage). To assess the level of agreement among independent radiologists in interpreting MRI signals, κ statistics were calculated for documented imaging variables.

To investigate the independent predictive factors for MVI, univariate logistic regression analysis was used to assess each variable in the training cohort. Stepwise multivariate analysis was performed on all variables associated with MVI at a significant level ($p < 0.05$), considering their clinical relevance into account as well. A nomogram was developed based on the results of multivariate logistic regression analysis and by using the “rms” package of R. It converted each regression coefficient into a 0–100 scale. A 100-point rating was assigned to the variable with the highest coefficient (absolute value). The total points were calculated based on the independent variables and then converted into predicted probabilities. The predictive performance of the nomogram was assessed based on its discrimination, calibration and clinical utility using 1000 bootstrap samples to reduce overfitting bias. The “pROC” package in R was used to plot the receiver operating characteristic (ROC) curve, and the “rmda” package was employed for decision curve analysis (DCA).

Nomograms were used for the clinical application of the model, and the total scores for each patient were calculated. For serum LCAT and CNDP1 level, the optimal cutoff values were determined using ROC curve analysis, which involved maximizing the Youden index (sensitivity + specificity – 1), with clinical applicability also taken into account.

In all analyses, $p < 0.05$ was considered statistically significant. SPSS version 21.0 (SPSS Inc.) and R version 4.2.2 (2022–10–31 ucrt, <http://www.r-project.org/>) were used for all data analyses. The data analysis was conducted from July 1st, 2023 to April 20th, 2024.

Results

Baseline characteristics of the patients

In this study, 260 patients were consecutively enrolled based on the inclusion criteria. These patients were randomly divided into a training cohort ($n = 182$) for nomogram development and a validation cohort ($n = 78$) to assess the performance of the model at a 7:3 ratio. Detailed

Table 1
Comparisons of patient characteristics in training and validation cohort.

Variable	Training (n = 182)	Validation (n = 78)	p Value
Age (y)	55.54 (49.00 – 63.00)	58.22 (51.75 – 66.00)	0.062
Sex			<0.001
Male	154 (84.6)	66 (84.6)	
Female	28 (15.4)	12 (15.4)	
Epidemic factor			0.993
HBV	132 (72.5)	54 (69.2)	
HCV	23 (12.6)	10 (12.8)	
Alcoholic	8 (4.4)	10 (12.8)	
Others	19 (10.4)	4 (5.1)	
Blood ammonia (μmol/L)			0.481
≤30	63 (42.6)	31 (47.4)	
>30	85 (57.4)	34 (52.3)	
PT (seconds)			0.520
≤16	177 (97.3)	77 (98.7)	
>16	5 (2.7)	1 (1.3)	
HBsAg			0.521
Negative	1 (0.8)	0 (0)	
Positive	131 (99.2)	54 (100)	
HBeAg			0.063
Negative	105 (79.5)	36 (66.7)	
Positive	27 (20.5)	18 (33.3)	
HBV DNA load (IU/mL)			0.611
≤10 ⁴	107 (81.1)	42 (77.8)	
>10 ⁴	25 (18.9)	12 (22.2)	
HCV RNA load (IU/mL)			0.511
≤100	20 (69.0)	11 (78.6)	
>100	9 (31.0)	3 (21.4)	
WBCs (x10 ⁹ /L)			0.581
<4	122 (67.0)	55 (70.5)	
≥4	60 (33.0)	23 (29.5)	
RBCs (x10 ¹² /L)	4.46 (4.08 – 4.79)	4.49 (4.03 – 4.81)	0.798
Platelets (x10 ⁹ /L)			0.509
<100	54 (29.7)	20 (25.6)	
≥100	128 (70.3)	58 (74.4)	
AFP (ng/mL)			0.196
≤20	94 (52.8)	48 (61.5)	
>20	84 (47.2)	30 (38.5)	
CA-125 (U/mL)			0.593
≤35	141 (84.9)	60 (82.2)	
>35	25 (15.1)	13 (17.8)	
CA-19-9 (U/mL)			0.524
≤39	133 (79.6)	57 (76.0)	
>39	34 (20.4)	18 (24.0)	
CEA (ng/mL)			0.472
≤4.7	144 (86.2)	62 (82.7)	
>4.7	23 (13.8)	13 (17.3)	
Albumin (g/L)			0.403
<35	146 (80.2)	66 (84.6)	
≥35	36 (19.8)	12 (15.4)	
TBil (μmol/L)			0.394
<34	171 (94.0)	71 (91.0)	
≥34	11 (6.0)	7 (9.0)	
ALT (U/L)			0.320
≤40	139 (76.4)	57 (73.1)	
>40	43 (23.6)	21 (26.9)	
AST (U/L)			0.932
≤40	120 (65.9)	51 (65.4)	
>40	62 (34.1)	27 (34.6)	
GGT (U/L)			0.422
≤64	107 (58.8)	50 (64.1)	
>64	75 (41.2)	28 (35.9)	
LCAT (ng/mL)			0.704
<203	84 (46.2)	38 (48.7)	
≥203	98 (53.8)	40 (51.3)	
CNDP1 (ng/mL)			0.075
<80	94 (59.1)	48 (71.6)	
≥80	65 (40.9)	19 (28.4)	
Antiviral therapy ^a			0.353
Yes	107 (58.8)	41 (52.6)	
No	75 (41.2)	37 (47.4)	
Cirrhosis			0.714
Yes	158 (86.8)	69 (88.5)	

(continued on next page)

Table 1 (continued)

Variable	Training (n = 182)	Validation (n = 78)	p Value
No	24 (13.2)	9 (11.5)	
Diabetes mellitus			0.653
Yes	33 (18.1)	16 (20.5)	
No	149 (81.9)	62 (79.5)	
Hepatic encephalopathy			0.320
Yes	4 (2.2)	0 (0)	
No	178 (97.8)	78 (100)	
Ascites			0.088
Yes	125 (68.7)	45 (57.7)	
No	57 (31.3)	33 (42.3)	
Hypertension			0.637
Yes	53 (29.1)	25 (32.1)	
No	129 (70.9)	53 (67.9)	
MVI			0.503
Presence	111 (61.0)	51 (65.4)	
Absence	71 (39.0)	27 (34.6)	
No. of tumors			0.391
solitary	113 (62.1)	44 (56.4)	
multiple	69 (37.9)	34 (43.6)	
Tumor diameter (cm)			0.477
≤3	81 (44.5)	31 (39.7)	
>3	101 (55.5)	47 (60.3)	
TNM classification (T)			0.211
T1	65 (35.7)	27 (34.6)	
T2	58 (31.9)	29 (37.2)	
T3	18 (9.9)	2 (2.6)	
T4	41 (22.5)	20 (25.6)	

Abbreviations: HBV, hepatitis B virus; HCV, hepatitis C virus; PT, prothrombin time; HBsAg, hepatitis B surface antigen; HBeAg, hepatitis B e antigen; HBV DNA, hepatitis B virus DNA; HCV RNA, hepatitis C virus RNA; WBCs, white blood cells; RBCs, red blood cells; AFP, α -fetoprotein; CA-125, carbohydrate antigen 125; CA-19-9, carbohydrate antigen 19-9; CEA, Carcinoembryonic antigen; TBil, total bilirubin; ALT, alanine aminotransferase; AST, aspartate aminotransferase; GGT, γ -glutamyl transpeptidase; LCAT, lecithin-cholesterol acyltransferase; CNDP1, carnosine dipeptidase 1; MVI, microvascular invasion.

^a Antiviral therapy was given before surgery.

Numbers are presented as medians (interquartile ranges) or frequency (percentages).

clinical characteristics of the 260 patients included in this study are listed in Table 1. Histopathologically identified MVI was identified in 111 (61.0 %) and 51 (65.4 %) patients in the two cohorts. The baseline clinicopathological data were similar in both the training and validation cohorts. No significant statistical differences were observed in these clinical characteristics between the two cohorts ($p = 0.062$ – 0.993), except for sex ($p < 0.001$).

Nomogram for MVI presence probability

All variables used in the analysis were based on preoperative data. Tumor-related variables, including tumor diameter, number, TNM classification, and liver cirrhosis, were assessed using preoperative imaging studies.

Univariate logistic analysis showed serum AFP (OR 2.588; 95 % CI 1.375–4.873; $p = 0.003$), CA-125 (OR 3.358; 95 % CI 1.094–10.303; $p = 0.034$), alanine aminotransferase ([ALT], OR 2.209; 95 % CI 1.030–4.738; $p = 0.042$), aspartate aminotransferase ([AST], OR 2.433; 95 % CI 1.241–4.767; $p = 0.010$), LCAT (OR 2.818; 95 % CI 1.505–5.277; $p = 0.001$), CNDP1 (OR 3.362; 95 % CI 1.735–6.516; $p < 0.001$), cirrhosis (OR 3.036; 95 % CI 1.249–7.380; $p = 0.014$), ascites (OR 2.272; 95 % CI 1.143–4.517; $p = 0.019$), number of tumor (OR 6.921; 95 % CI 3.219–14.882; $p < 0.001$) and tumor diameter (OR 6.885; 95 % CI 3.539–13.394; $p < 0.001$), may be significantly related to MVI ($p < 0.05$). Therefore, we incorporated these variables into the multivariate regression equation for further analysis. The results of univariate analysis of the presence of MVI based on preoperative data in the training cohort are shown in Table 2. Multivariate analysis revealed that low serum CNDP1 (< 80 ng/mL) (OR 2.973; 95 % CI 1.167–7.575; p

Table 2

Univariate logistic analysis results in the training cohort.

Variable	OR(95 % CI)	p Value
Age (y)	0.995 (0.965 - 1.025)	0.738
Sex, male vs female	1.702 (0.757 - 3.825)	0.198
Epidemic factor		0.580
HCV vs HBV	1.533 (0.591 - 3.981)	0.380
Alcoholic vs HBV	2.013 (0.391 - 10.352)	0.403
Others vs HBV	0.745 (0.284 - 1.957)	0.551
Blood ammonia, >30 vs ≤30 (μmol/L)	1.153 (0.578 - 2.299)	0.687
PT	2.617 (0.287 - 23.900)	0.394
WBCs, <4 vs ≥4 ($\times 10^9/L$)	1.159(0.613 - 2.194)	0.649
RBCs ($\times 10^{12}/L$)	0.731 (0.444 - 1.201)	0.216
Platelets, <100 vs ≥100 ($\times 10^9/L$)	1.413 (0.726 - 2.752)	0.309
AFP, >20 vs ≤20 (ng/mL)	2.588 (1.375 - 4.873)	0.003 [#]
CA-125, >35 vs ≤35 (U/mL)	3.358 (1.094 - 10.303)	0.034 [#]
CA-19-9, >39 vs ≤39 (U/mL)	1.446 (0.639 - 3.272)	0.376
CEA, >4.7 vs ≤4.7 (ng/mL)	0.691 (0.283 - 1.689)	0.418
Albumin, <35 vs ≥35 (g/L)	1.866 (0.838 - 4.153)	0.127
ALT, >40 vs ≤40 (U/L)	2.209 (1.030 - 4.738)	0.042 [#]
AST, >40 vs ≤40 (U/L)	2.433 (1.241 - 4.767)	0.010 [#]
GGT, >64 vs ≤64 (U/L)	1.665 (0.898 - 3.086)	0.106
LCAT, <203 vs ≥203 (ng/mL)	2.818 (1.505 - 5.277)	0.001 [#]
CNDP1, <80 vs ≥80 (ng/mL)	3.362 (1.735 - 6.516)	<0.001 [#]
Antiviral therapy, yes vs no ^a	0.544 (0.292 - 1.012)	0.055
Cirrhosis, yes vs no	3.036 (1.249 - 7.380)	0.014 [#]
Diabetes mellitus, yes vs no	0.535 (0.250 - 1.144)	0.107
Ascites, yes vs no	2.272 (1.143 - 4.517)	0.019 [#]
Hypertension, yes vs no	0.773 (0.404 - 1.481)	0.437
No. of tumors, multiple vs solitary	6.921 (3.219 - 14.882)	<0.001 [#]
Tumor diameter, >3 vs ≤3 (cm)	6.885 (3.539 - 13.394)	<0.001 [#]

Abbreviations: OR, odds ratio; CI, confidence interval; HBV, hepatitis B virus; HCV, hepatitis C virus; PT, prothrombin time; WBCs, white blood cells; RBCs, red blood cells; AFP, α -fetoprotein; CA-125, carbohydrate antigen 125; CA-19-9, carbohydrate antigen 19-9; CEA, Carcinoembryonic antigen; ALT, alanine aminotransferase; AST, aspartate aminotransferase; GGT, γ -glutamyl transpeptidase; LCAT, lecithin-cholesterol acyltransferase; CNDP1, carnosine dipeptidase 1; MVI, microvascular invasion.

^a Antiviral therapy was given before surgery.

[#] Indicates $p < 0.05$.

= 0.022), cirrhosis (OR 8.911; 95 % CI 1.922–41.318; $p = 0.005$); multiple tumors (OR 4.095; 95 % CI 1.374–12.205; $p = 0.011$), and tumor diameter ≥ 3 cm (OR 4.408; 95 % CI 1.780–10.919; $p = 0.001$) were independent predictors of MVI (Table 3).

The prediction model combining serum CNDP1 levels, cirrhosis, tumor number and diameter contributed more ($p < 0.05$) to MVI in the multivariate logistic regression analysis. A nomogram based on the multivariate model was built to preoperatively predict the risk of MVI for each individual (Fig. 1).

Table 3

Multivariate logistic analysis results in the training cohort.

Variable	β^a	OR(95 % CI)	p Value
AFP, >20 vs ≤20 (ng/mL)	0.664	1.942 (0.734 - 5.135)	0.181
CA-125, >35 vs ≤35 (U/mL)	-0.379	0.684 (0.138 - 3.406)	0.643
ALT, >40 vs ≤40 (U/L)	0.569	1.766 (0.415 - 7.521)	0.442
AST, >40 vs ≤40 (U/L)	-0.346	0.708 (0.187 - 2.678)	0.611
LCAT, <203 vs ≥203 (ng/mL)	0.852	2.345 (0.894 - 6.150)	0.083
CNDP1, <80 vs ≥80 (ng/mL)	1.090	2.973 (1.167 - 7.575)	0.022 [*]
Cirrhosis, yes vs no	2.187	8.911 (1.922 - 41.318)	0.005 [*]
Ascites, yes vs no	-0.069	0.933 (0.301 - 2.896)	0.904
No. of tumors, multiple vs solitary	1.410	4.095 (1.374 - 12.205)	0.011 [*]
Tumor diameter, ≥ 3 vs <3 (cm)	1.483	4.408 (1.780 - 10.919)	0.001 [*]
Constant	-3.847	0.021	<0.001

Abbreviations: OR, odds ratio; CI, confidence interval; AFP, α -fetoprotein; CA-19-9, carbohydrate antigen 19-9; LCAT, lecithin-cholesterol acyltransferase; CNDP1, carnosine dipeptidase 1; MVI, microvascular invasion.

^a Unstandardized β coefficients were calculated from the multivariate logistic regression model.

^{*} Indicates $p < 0.05$.

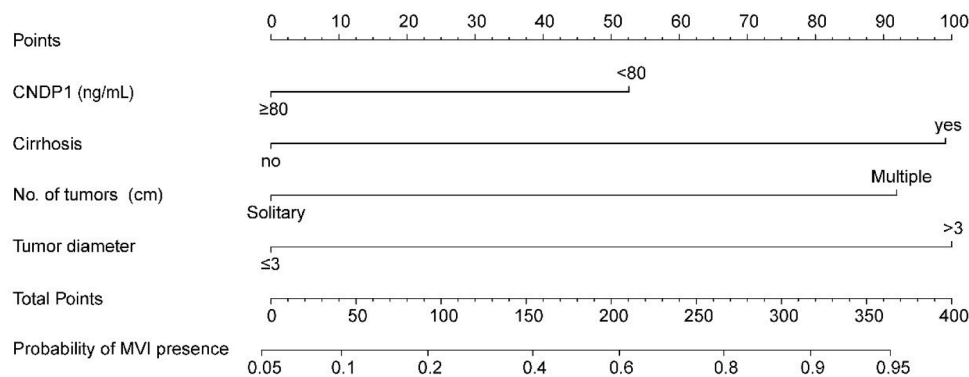


Fig. 1. Nomogram to estimate the risk of MVI presence preoperatively in HCC

The prediction model combined serum CNDP1 levels, cirrhosis, number of tumor and tumor diameter. The nomogram can be used by determining the position of each variable on the corresponding axis, drawing a line to the point axis, and adding points from all variables. Next, a line was drawn from the total point axis to determine MVI probabilities using the bottom line of the nomogram.

CNDP1, carnosine dipeptidase 1; MVI, microvascular invasion.

Validation and efficacy evaluation of the nomogram

The nomogram showed good predictive performance in estimating the risk of MVI, with a C-index of 0.833 (95 % CI 0.771–0.894) in the training cohort and 0.821 (95 % CI 0.720–0.922) in the validation cohort (Fig. 2A, B). Calibration plots graphically showed satisfactory agreement in the presence of MVI between the risk estimated by the nomogram and the actual MVI estimates in both cohorts. (Fig. 2C, D).

The decision curve for the nomogram in the two datasets is shown in Fig. 2E and F. The net benefit derived from the decision curve of the predictive nomogram was higher than the benefit that would be achieved by assuming all patients in both cohorts had MVI. Our nomogram indicates that a therapeutic strategy based on its predictions would improve clinical outcomes.

Discussion

HCC patients with MVI have a poor prognosis due to intrahepatic and distant tumor spread [9,10,31,32]. In this study, by integrating clinicopathologic and clinicoradiological characteristics, we developed and validated a nomogram for predicting MVI in HCC patients preoperatively. Initially, various baseline patient characteristics were examined using univariate logistic regression analysis within the training dataset. The univariate logistic analysis indicated that serum AFP, CA-125, ALT, AST, LCAT and CNDP1 levels, cirrhosis, ascites, tumor number and diameter were significantly associated with MVI ($p < 0.05$). Subsequently, the aforementioned variables were integrated into the multivariate logistic regression equation, revealing low serum CNDP1 (< 80 ng/mL), cirrhosis, multiple tumors, and tumor diameter ≥ 3 cm were independent predictive factors for MVI ($p < 0.05$).

Furthermore, we developed and validated a predictive model that incorporated serum CNDP1 level, cirrhosis, tumor number, and tumor diameter, which exhibited a discrimination of 0.833 in the training cohort and 0.821 in the validation cohort for preoperative prediction of MVI. Moreover, to provide a visual representation of the highly accurate model, we constructed a nomogram as an evaluative instrument in the present study. Its clinical significance was subsequently validated through decision curve analysis.

Previous research has endeavored to employ preoperative imaging alongside serum and tumorous biomarkers for predicting MVI; however, additional clinical validation is imperative [9]. A study was conducted to investigate the utilization of an artificial neural network model for the purpose of preoperative risk estimation of MVI, incorporating three key factors: number of tumors, diameter, and serum AFP level [33]. However, other factors, including tumor biomarkers, which may be related to MVI, were not included in the model [9]. Moreover, the use of this

model necessitates the utilization of specialized computer software, rendering it incompatible with handheld device software, thereby constraining its widespread applicability. Among the existing prognostic instruments, a nomogram exhibits notable precision and discriminative attributes in predicting outcomes and is convenient to use during clinical work [34]. The number of tumors, tumor diameter, and serum AFP level were also found to be related to MVI in patients with HCC and the living-donor liver transplantation population [15,16,32,35]. Some studies have discovered that cirrhosis served as an independent predictive factor for MVI in HCC patients [36–38], which was consistent with the finding of our study.

To enhance the reliability of the MVI prediction model in HCC patients, it is advisable to simultaneously consider clinicopathological data, imaging parameters, and specific biomarkers. Previously, through bioinformatics analysis and clinical sample validation, we identified these two potential HCC biomarkers as weakly expressed in HCC. Our findings implied that LCAT and CNDP1 levels, particularly CNDP1, may hold a comparatively significant position in predicting the existence of MVI in HCC. To our knowledge, this study is the first attempt to incorporate these two variables into a nomogram for predicting MVI. Consequently, our study expands the prospective application of biomarkers in preoperative prediction of MVI.

The present study has certain limitations. Firstly, this was a single-center retrospective study with a limited sample size. Therefore, it is imperative to conduct additional prospective validations using larger cohorts from multiple institutions to enhance the reliability of our findings. Secondly, previous studies have explored the amalgamation of diverse gene characteristics to enhance the precision of predicting MVI in HCC [39–41], our study did not include the genomic factors associated with MVI. However, the excessive expenses associated with multi-gene expression assays and intricate technological requirements pose challenges in implementing genomics for routine clinical settings, currently.

In conclusion, the development of a nomogram incorporating four preoperative risk factors for MVI in HCC allows patients to effectively assess their MVI risk before undergoing surgery, thereby providing potential clinical benefits.

CRediT authorship contribution statement

Xiao-Wen Huang: Formal analysis, Writing – original draft, Writing – review & editing, Methodology, Software. **Yan Li:** Data curation, Investigation, Methodology. **Li-Na Jiang:** Methodology, Project administration, Writing – review & editing. **Bo-Kang Zhao:** Data curation, Resources. **Yi-Si Liu:** Resources. **Chun Chen:** Data curation. **Dan Zhao:** Data curation. **Xue-Li Zhang:** Data curation, Resources. **Mei-Ling Li:** Resources. **Yi-Yun Jiang:** Resources. **Shu-Hong Liu:** Resources. **Li**

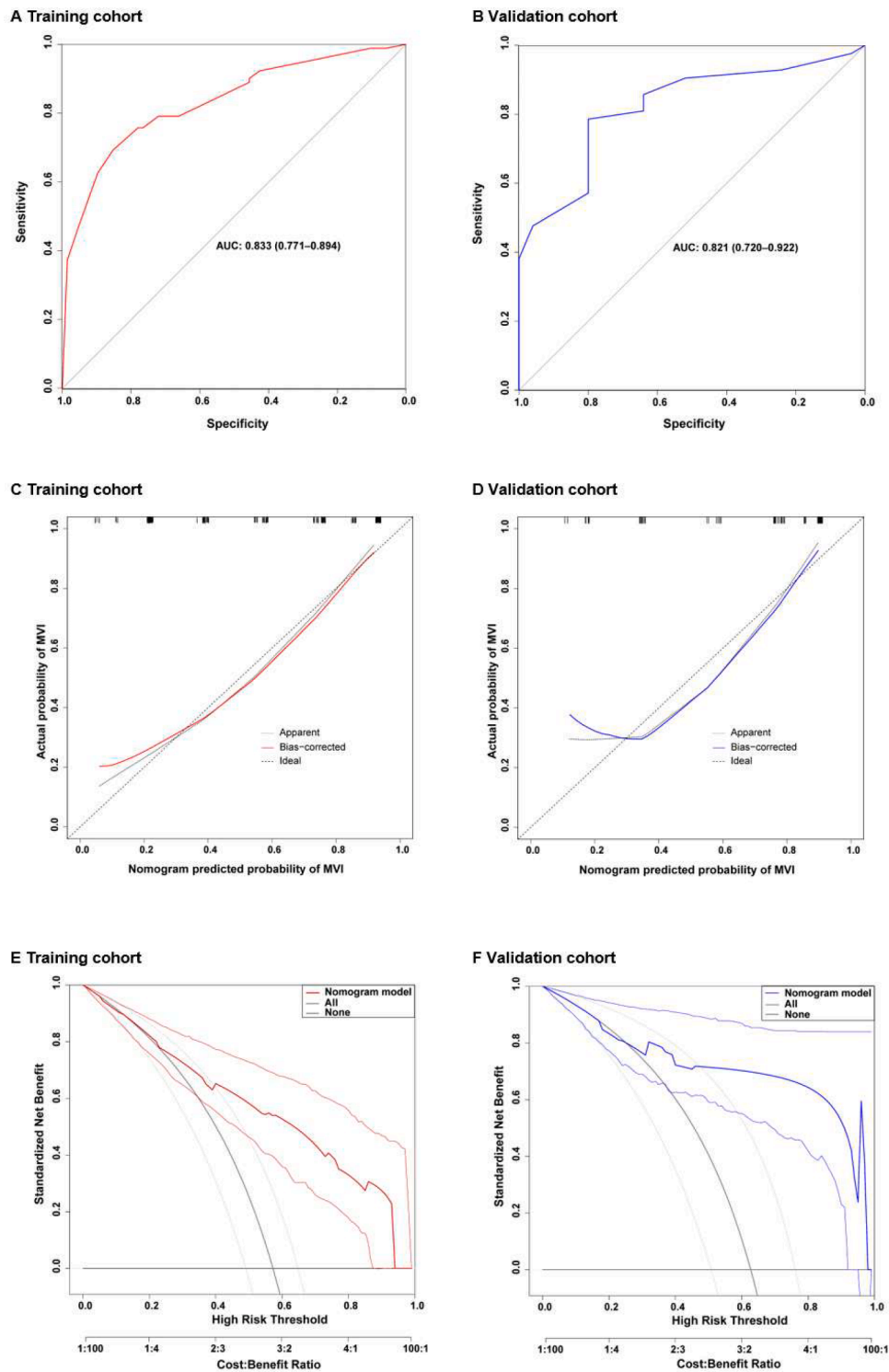


Fig. 2. Validity of the predictive performance of the nomogram in estimating the risk of MVI presence
A, ROC curve in the training cohort based on the prediction model ($n = 182$). **B,** ROC curve of the validation cohort based on the prediction model ($n = 78$).
C, Calibration curve of the training cohort based on the prediction model ($n = 182$).
D, Calibration curve of the validation cohort based on the prediction model ($n = 78$). The X-axis represents the probability of MVI predicted by a nomogram, the y-axis represents the observed MVI, and the diagonal dashed line represents the ideal prediction by a perfect model.
E, Decision curve in the training cohort based on the prediction model ($n = 182$). The black line represents the net benefit of assuming that all patients have MVI, the gray line represents the net benefit of not assuming that any patients have MVI, and the red line represents the expected net benefit per patient based on the predictive nomogram.
F, Decision curve in the validation cohort based on the prediction model ($n = 78$). The black line represents the net benefit of assuming that all patients have MVI, the gray line represents the net benefit of not assuming that any patients have MVI, and the blue line represents the expected net benefit per patient based on the predictive nomogram.
 AUC, area under the curve; MVI, microvascular invasion.

Zhu: Resources. **Jing-Min Zhao:** Supervision, Funding acquisition, Project administration, Writing – review & editing.

Declaration of competing interest

The authors declare that they have no known competing financial interests or personal relationships that could have appeared to influence the work reported in this paper.

Funding

This study was supported by National Key Research and Development Program of China (2023YFC2308104), General Program of the National Natural Science Foundation of China (81673654) and the National Key Clinical Specialist Army Construction Project (the Former General Logistics Department Healthcare No. 2016–1).

Ethics approval

This study was approved by the Institutional Ethics Committee of the Fifth Medical Center of Chinese PLA General Hospital (authorization number: 2020055D). All research was conducted in accordance with both the Declarations of Helsinki and Istanbul. Informed consent was obtained from all patients for the data to be used in the study. The patient did not receive any financial compensation.

Acknowledgments

We thank the numerous participants and providers who were involved in this study.

References

- H. Sung, J. Ferlay, R.L. Siegel, M. Laversanne, I. Soerjomataram, A. Jemal, F. Bray, Global cancer statistics 2020: GLOBOCAN estimates of incidence and mortality worldwide for 36 cancers in 185 countries, *CA Cancer J. Clin.* 71 (2021) 209–249.
- J. Bruix, J.M. Llovet, Major achievements in hepatocellular carcinoma, *Lancet* 373 (2009) 614–616.
- S.T. Fan, C. Mau Lo, R.T. Poon, C. Yeung, C. Leung Liu, W.K. Yuen, C. Ming Lam, K. K. Ng, S. Ching Chan, Continuous improvement of survival outcomes of resection of hepatocellular carcinoma: a 20-year experience, *Ann. Surg.* 253 (2011) 745–758.
- J.M. Llovet, M. Schwartz, V. Mazzaferro, Resection and liver transplantation for hepatocellular carcinoma, *Semin. Liver Dis.* 25 (2005) 181–200.
- A. Saito, H. Toyoda, M. Kobayashi, Y. Koiwa, H. Fujii, K. Fujita, A. Maeda, Y. Kaneoka, S. Hazama, H. Nagano, A.H. Mirza, H.P. Graf, E. Cosatto, Y. Murakami, M. Kuroda, Prediction of early recurrence of hepatocellular carcinoma after resection using digital pathology images assessed by machine learning, *Mod. Pathol.* 34 (2021) 417–425.
- R. De Angelis, M. Sant, M.P. Coleman, S. Francisci, P. Baili, D. Pierannunzio, A. Trama, O. Visser, H. Brenner, E. Ardanaz, M. Bielska-Lasota, G. Engholm, A. Nennecke, S. Siesling, F. Berrino, R. Capocaccia, Cancer survival in Europe 1999–2007 by country and age: results of EURO-CARE–5—a population-based study, *Lancet Oncol.* 15 (2014) 23–34.
- W.M. Cong, H. Bu, J. Chen, H. Dong, Y.Y. Zhu, L.H. Feng, J. Chen, Practice guidelines for the pathological diagnosis of primary liver cancer: 2015 update, *World J. Gastroenterol.* 22 (2016) 9279–9287.
- S. Roayaie, I.N. Blume, S.N. Thung, M. Guido, M.I. Fiel, S. Hiotis, D.M. Labow, J. M. Llovet, M.E. Schwartz, A system of classifying microvascular invasion to predict outcome after resection in patients with hepatocellular carcinoma, *Gastroenterology* 137 (2009) 850–855.
- M. Rodríguez-Perálvarez, T.V. Luong, L. Andreana, T. Meyer, A.P. Dhillon, A. K. Burroughs, A systematic review of microvascular invasion in hepatocellular carcinoma: diagnostic and prognostic variability, *Ann. Surg. Oncol.* 20 (2013) 325–339.
- K.C. Lim, P.K. Chow, J.C. Allen, G.S. Chia, M. Lim, P.C. Cheow, A.Y. Chung, L. L. Ooi, S.B. Tan, Microvascular invasion is a better predictor of tumor recurrence and overall survival following surgical resection for hepatocellular carcinoma compared to the Milan criteria, *Ann. Surg.* 254 (2011) 108–113.
- S. Hwang, Y.J. Lee, K.H. Kim, C.S. Ahn, D.B. Moon, T.Y. Ha, G.W. Song, D.H. Jung, S.G. Lee, The impact of tumor size on long-term survival outcomes after resection of solitary hepatocellular carcinoma: single-institution experience with 2558 patients, *J. Gastrointest. Surg.* 19 (2015) 1281–1290.
- M. Shi, R.P. Guo, X.J. Lin, Y.Q. Zhang, M.S. Chen, C.Q. Zhang, W.Y. Lau, J.Q. Li, Partial hepatectomy with wide versus narrow resection margin for solitary hepatocellular carcinoma: a prospective randomized trial, *Ann. Surg.* 245 (2007) 36–43.
- V. Mazzaferro, J.M. Llovet, R. Miceli, S. Bhoori, M. Schiavo, L. Mariani, T. Camerini, S. Roayaie, M.E. Schwartz, G.L. Grazi, R. Adam, P. Neuhaus, M. Salizzoni, J. Bruix, A. Forner, L. De Carlis, U. Cillo, A.K. Burroughs, R. Troisi, M. Rossi, G.E. Gerunda, J. Lerut, J. Belghiti, I. Boin, J. Gugenheim, F. Rochling, B. Van Hoek, P. Majno, Predicting survival after liver transplantation in patients with hepatocellular carcinoma beyond the Milan criteria: a retrospective, exploratory analysis, *Lancet Oncol.* 10 (2009) 35–43.
- A.S. Gouw, C. Balabaud, H. Kusano, S. Todo, T. Ichida, M. Kojiro, Markers for microvascular invasion in hepatocellular carcinoma: where do we stand? *Liver Transpl.* 17 (2) (2011) S72–S80. Suppl.
- Z. Lei, J. Li, D. Wu, Y. Xia, Q. Wang, A. Si, K. Wang, X. Wan, W.Y. Lau, M. Wu, F. Shen, Nomogram for preoperative estimation of microvascular invasion risk in hepatitis B Virus-related hepatocellular carcinoma within the milan criteria, *JAMA Surg.* 151 (2016) 356–363.
- P.P. McHugh, J. Gilbert, S. Vera, A. Koch, D. Ranjan, R. Gedaly, Alpha-fetoprotein and tumour size are associated with microvascular invasion in explanted livers of patients undergoing transplantation with hepatocellular carcinoma, *HPB (Oxford)* 12 (2010) 56–61.
- X. Zhao, Y. Wang, H. Xia, S. Liu, Z. Huang, R. He, L. Yu, N. Meng, H. Wang, J. You, J. Li, J.W.P. Yam, Y. Xu, Y. Cui, Roles and molecular mechanisms of biomarkers in hepatocellular carcinoma with microvascular invasion: a review, *J. Clin. Transl. Hepatol.* 11 (2023) 1170–1183.
- H. Hu, Q. Zheng, Y. Huang, X.W. Huang, Z.C. Lai, J. Liu, X. Xie, S.T. Feng, W. Wang, M. Lu, A non-smooth tumor margin on preoperative imaging assesses microvascular invasion of hepatocellular carcinoma: a systematic review and meta-analysis, *Sci. Rep.* 7 (2017) 15375.
- M. Renzulli, S. Brocchi, A. Cucchetti, F. Mazzotti, C. Mosconi, C. Sportoletti, G. Brandi, A.D. Pinna, R. Golfieri, Can current preoperative imaging be used to detect microvascular invasion of hepatocellular carcinoma? *Radiology* 279 (2016) 432–442.
- X. Peng, Z. Chen, F. Farshidfar, X. Xu, P.L. Lorenzi, Y. Wang, F. Cheng, L. Tan, K. Mojumdar, D. Du, Z. Ge, J. Li, G.V. Thomas, K. Birsoy, L. Liu, H. Zhang, Z. Zhao, C. Marchand, J.N. Weinstein, O.F. Bathe, H. Liang, Molecular characterization and clinical relevance of metabolic expression subtypes in human cancers, *Cell Rep.* 23 (2018) 255–269, e254.
- G. Pascual, A. Avgustinova, S. Mejetta, M. Martín, A. Castellanos, C.S. Attolini, A. Berenguer, N. Prats, A. Toll, J.A. Hueto, C. Bescós, L. Di Croce, S.A. Benitah, Targeting metastasis-initiating cells through the fatty acid receptor CD36, *Nature* 541 (2017) 41–45.
- D.E. Piper, W.G. Romanow, R.N. Gunawardane, P. Fordstrom, S. Masterman, O. Pan, S.T. Thibault, R. Zhang, D. Meininger, M. Schwarz, Z. Wang, C. King, M. Zhou, N.P. Walker, The high-resolution crystal structure of human LCAT, *J. Lipid Res.* 56 (2015) 1711–1719.
- A.B. Kosek, D. Durbin, A. Jonas, Binding affinity and reactivity of lecithin cholesterol acyltransferase with native lipoproteins, *Biochem. Biophys. Res. Commun.* 258 (1999) 548–551.
- M.A. Clay, D.H. Pyle, K.A. Rye, P.J. Barter, Formation of spherical, reconstituted high density lipoproteins containing both apolipoproteins A-I and A-II is mediated by lecithin:cholesterol acyltransferase, *J. Biol. Chem.* 275 (2000) 9019–9025.
- K. Yang, J. Wang, H. Xiang, P. Ding, T. Wu, G. Ji, LCAT- targeted therapies: progress, failures and future, *Biomed. Pharmacother.* 147 (2022) 112677.
- P. Icard, L. Fournel, Z. Wu, M. Alifano, H. Lincet, Interconnection between metabolism and cell cycle in cancer, *Trends Biochem. Sci.* 44 (2019) 490–501.
- P. Pandya, M.K. Ekka, R.K. Dutta, S. Kumaran, Mass spectrometry assay for studying kinetic properties of dipeptidases: characterization of human and yeast dipeptidases, *Anal. Biochem.* 418 (2011) 134–142.
- J.F. Lenney, R.P. George, A.M. Weiss, C.M. Kucera, P.W. Chan, G.S. Rinzler, Human serum carnosinase: characterization, distinction from cellular carnosinase, and activation by cadmium, *Clin. Chim. Acta* 123 (1982) 221–231.
- S.L. Chen, T. Marino, W.H. Fang, N. Russo, F. Himo, Peptide hydrolysis by the binuclear zinc enzyme aminopeptidase from *Aeromonas proteolytica*: a density functional theory study, *J. Phys. Chem. B* 112 (2008) 2494–2500.
- A. Toyosaka, E. Okamoto, M. Mitsunobu, T. Oriyama, N. Nakao, K. Miura, Pathologic and radiographic studies of intrahepatic metastasis in hepatocellular carcinoma; the role of efferent vessels, *HPB surgery: a world journal of hepatic, pancreatic and biliary surgery, discussion* 10 (1996) 103–104, 97–103.
- M. Ziol, N. Poté, G. Amaddeo, A. Laurent, J.C. Nault, F. Oberti, C. Costentin, S. Michalak, M. Bouattour, C. Francoz, G.P. Pageaux, J. Ramos, T. Decaens, A. Luciani, B. Guiu, V. Vilgrain, C. Aubé, J. Derman, C. Charpy, J. Zucman-Rossi, N. Barget, O. Seror, N. Ganne-Carrié, V. Paradis, J. Calderaro, Macrotrabecular-massive hepatocellular carcinoma: a distinctive histological subtype with clinical relevance, *Hepatology* 68 (2018) 103–112.
- T. Iguchi, K. Shirabe, S. Aishima, H. Wang, N. Fujita, M. Ninomiya, Y. Yamashita, T. Ikegami, H. Uchiyama, T. Yoshizumi, Y. Oda, Y. Maehara, New pathologic stratification of microvascular invasion in hepatocellular carcinoma: predicting prognosis after living-donor liver transplantation, *Transplantation* 99 (2015) 1236–1242.
- A. Cucchetti, F. Piscaglia, A.D. Grigioni, M. Ravaioli, M. Cescon, M. Zanello, G. L. Grazi, R. Golfieri, W.F. Grigioni, A.D. Pinna, Preoperative prediction of hepatocellular carcinoma tumour grade and micro-vascular invasion by means of artificial neural network: a pilot study, *J. Hepatol.* 52 (2010) 880–888.
- S.F. Shariat, U. Capitano, C. Jeldres, P.I. Karakiewicz, Can nomograms be superior to other prediction tools? *BJU Int.* 103 (2009) 495–497, 492–495; discussion.
- H. Zhao, Y. Hua, Z. Lu, S. Gu, L. Zhu, Y. Ji, Y. Qiu, T. Dai, H. Jin, Prognostic value and preoperative predictors of microvascular invasion in solitary hepatocellular

- carcinoma \leq 5 cm without macrovascular invasion, *Oncotarget* 8 (2017) 61203–61214.
- [36] X.C. Mao, S. Shi, L.J. Yan, H.C. Wang, Z.N. Ding, H. Liu, G.Q. Pan, X. Zhang, C. L. Han, B.W. Tian, D.X. Wang, S.Y. Tan, Z.R. Dong, Y.C. Yan, T. Li, A model based on adipose and muscle-related indicators evaluated by CT images for predicting microvascular invasion in HCC patients, *Biomark. Res.* 11 (2023) 87.
- [37] L. Wang, B. Feng, D. Li, M. Liang, S. Wang, S. Wang, X. Ma, X. Zhao, Risk stratification of solitary hepatocellular carcinoma \leq 5 cm without microvascular invasion: prognostic values of MR imaging features based on LI-RADS and clinical parameters, *Eur. Radiol.* 33 (2023) 3592–3603.
- [38] Y. Chang, T. Guo, B. Zhu, Y. Liu, A novel nomogram for predicting microvascular invasion in hepatocellular carcinoma, *Ann. Hepatol.* 28 (2023) 101136.
- [39] S. Banerjee, D.S. Wang, H.J. Kim, C.B. Sirlin, M.G. Chan, R.L. Korn, A.M. Rutman, S. Siripongsakun, D. Lu, G. Imanbayev, M.D. Kuo, A computed tomography radiogenomic biomarker predicts microvascular invasion and clinical outcomes in hepatocellular carcinoma, *Hepatology* 62 (2015) 792–800.
- [40] Y. Tang, L. Xu, Y. Ren, Y. Li, F. Yuan, M. Cao, Y. Zhang, M. Deng, Z. Yao, Identification and validation of a prognostic model based on three MVI-related genes in hepatocellular carcinoma, *Int. J. Biol. Sci.* 18 (2022) 261–275.
- [41] A. Beaufrère, S. Caruso, J. Calderaro, N. Poté, J.C. Bijot, G. Couchy, F. Cauchy, V. Vilgrain, J. Zucman-Rossi, V. Paradis, Gene expression signature as a surrogate marker of microvascular invasion on routine hepatocellular carcinoma biopsies, *J. Hepatol.* 76 (2022) 343–352.